MOF Membranes

DOI: 10.1002/anie.201104383

An Organophilic Pervaporation Membrane Derived from Metal–Organic Framework Nanoparticles for Efficient Recovery of Bio-Alcohols**

Xin-Lei Liu, Yan-Shuo Li, Guang-Qi Zhu, Yu-Jie Ban, Long-Ya Xu, and Wei-Shen Yang**

Metal–organic frameworks (MOFs) are novel hybrid inorganic–organic materials consisting of metal ions or clusters interconnected by a variety of organic compounds.[1] Their versatile architectures and customizable chemical functionalities make MOFs attractive candidates for constructing separating membranes with high performance.[2–4] A number of excellent advancements in fabricating molecular sieve membranes based on MOFs have been made in recent years.[3a–g, 4a] Unlike traditional inorganic zeolites with "rigid" frameworks, MOFs are in general structurally flexible, which is generally used to explain the absence of a clear cut-off, as expected from the pore size estimated from rigid framework models.[3a] On the other hand, this dynamic structural behavior of the MOFs is beneficial when elasticity is favorable, for example, in adsorption-based separation,[2a] because such flexible materials can exhibit high selectivity for guest inclusion by adapting their framework structure accordingly.

Recently, zeolitic imidazolate frameworks (ZIFs), a subfamily of MOFs, received tremendous attention because of their exceptional thermal and chemical stability.[5] One particularly interesting member of this family is ZIF-8 (with the formula zinc(2-methylimidazolate)$_2$).[6] ZIF-8 represents an appropriate model system and has found many applications, including selective adsorption,[7] membrane-based separation,[3a,b,g,i, 4a–c] chromatography,[8] catalysis,[9] and as a sensor.[10] In contrast to the hydrothermal synthesis of nanozeolites (e.g. silicalite-1) at high temperature and autogenous pressure, the preparation of ZIF-8 nanoparticles can be conducted at room temperature in solution, which is lower cost, saves time, and much more convenient.[11] Moreover, the superhydrophobicity of ZIF-8 results in it showing no adsorption of water before the onset of capillary condensation.[12] All the above-mentioned characteristics suggest that ZIF-8 nanoparticles could be used as fillers in mixed-matrix membranes (MMMs) for the recovery of organic compounds from aqueous solutions by adopting organophilic pervaporation (OPV) technology. Pervaporation is a membrane process based on a sorption–diffusion mechanism, and is considered the most promising technology for molecular-scale liquid/liquid separations.[13] Herein we show that both pervaporation selectivity and membrane flux of a silicone rubber membrane can be remarkably improved by doping ZIF-8 nanoparticles, which create preferential pathways for the permeation of organic compounds.

Preferential adsorption of a permeating organic species determines to a large extent its overall selectivity for OPV. To this end, an experimental and simulation study was performed to evaluate the adsorption properties of ZIF-8 nanoparticles toward bio-alcohols, in particular, isobutanol (next generation biofuels). Although the aperture size of ZIF-8 is estimated to be 0.34 nm,[5] an exceptional high capacity for isobutanol (kinetic diameter 0.50 nm[14]) was measured for the ZIF-8 nanoparticles, thus indicating a very flexible rather than a rigid framework structure. Figure 1a shows the adsorption isotherm for isobutanol with ZIF-8 nanoparticles (see Figures S1–S3 in the Supporting Information) at 40 °C obtained using an Intelligent Gravimetric Analyzer (IGA). The isotherm can be categorized as type V, with an extraordinary plateau value of around 360 mg g^{-1} at 3.5 kPa. This value is about four times that of the popular organophilic silicalite-1 nanoparticles.[15] In addition, a gate-opening effect[16] was observed at 0.5 kPa. Similar adsorption hysteresis has been observed experimentally in other types of flexible MOFs,[16b,c] where specific threshold pressures control the uptake and release of large individual molecules. Another interesting observation is the incomplete desorption, as evidenced from the desorption isotherm (Figure 1a). As proved by FTIR-ATR (see Figure S4 in the Supporting Information), the residual isobutanol can be completely desorbed by increasing the desorption temperature from 40 to 80 °C. This finding indicates that besides pressure dependence, the gate opening can also be triggered by temperature. In the current study, no phase transformation was observed during the desorption of isobutanol, as determined by XRD (see Figure S5 in the Supporting Information), thus indicating that unlocking the openings to the cavities (sodalite cages) of ZIF-8 might occur by rotation of the methylimidazole linkers. Similar to the report from other researchers,[12] our independent measurements (Figure 1a) show that the ZIF-8 nanoparticles, because

[*] X.-L. Liu, Prof. Dr. Y.-S. Li, Dr. G.-Q. Zhu, Y.-J. Ban, Prof. Dr. L.-Y. Xu, Prof. Dr. W.-S. Yang
State Key Laboratory of Catalysis
Dalian Institute of Chemical Physics, CAS
Zhongshan Road 457, 116023, Dalian (China)
E-mail: leeys@dicp.ac.cn
yangws@dicp.ac.cn
X.-L. Liu, Y.-J. Ban
Graduate School of Chinese Academy of Sciences
Beijing 100049 (China)

[**] This work was supported by the National Science Fund for Distinguished Young Scholars (20725313), the National Science Fund (21006101), and the DICP Independent Research Project (no. R201006).

Supporting information for this article is available on the WWW under http://dx.doi.org/10.1002/anie.201104383.

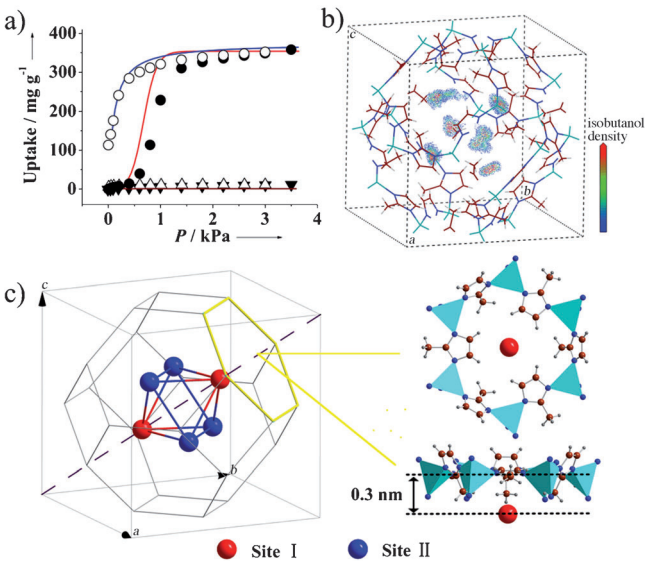

Figure 1. a) Experimental and simulated adsorption and desorption isotherms for isobutanol and water with ZIF-8 at 40 °C (filled (empty) circles and red (blue) lines represent experimental and simulated isobutanol adsorption (desorption); filled (empty) triangles represent experimental water adsorption (desorption), and the wine line simulated water adsorption; b) density contours for isobutanol in one sodalite cage of ZIF-8 at 3.5 kPa and 40 °C; c) representations of isobutanol adsorption sites in ZIF-8 (abstracted from (b)).

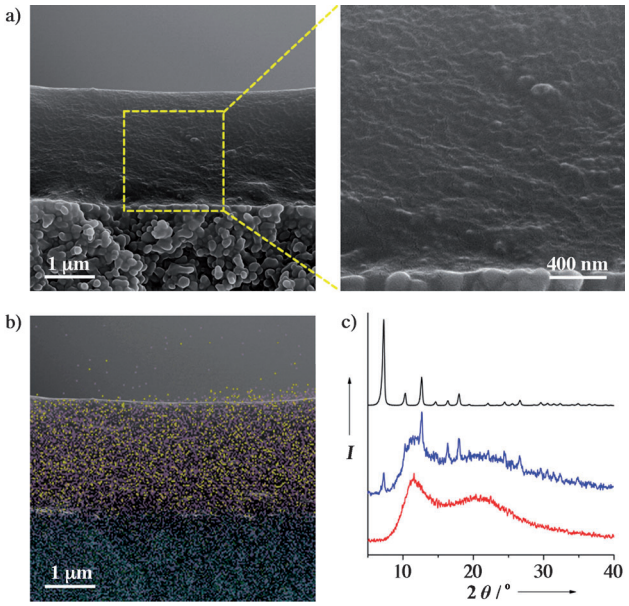

Figure 2. a) Cross-sectional SEM images and b) EDXS mapping of the ZIF-8-PMPS membrane ($W_{ZIF\text{-}8}/W_{PMPS} = 0.10{:}1$; Zn signal: yellow; Al signal: cyan; Si signal: pink); c) XRD patterns of ZIF-8 nanoparticles (black line), pure PMPS membrane (red line) and ZIF-8-PMPS membrane (blue line).

of their superhydrophobicity, exhibit no adsorption of water before the onset of capillary condensation.

Configurational bias grand canonical Monte Carlo (CB-GCMC)[17] simulations were performed to obtain a better understanding of the adsorption. The van der Waals and electrostatic interactions between the ZIF-8 framework and the isobutanol (or water) molecules were generated by employing the universal force field (UFF)[18] and the charge equilibration (QEq) algorithm.[19] The simulation results (both the adsorption and desorption branches, Figure 1a) are in reasonably good agreement with the experimental data, thereby indicating that the model and the UFF parameters used are suitable for describing the adsorption behavior of isobutanol in ZIF-8. Figure 1b shows the simulated density contours of isobutanol in one sodalite cage of ZIF-8 at 3.5 kPa and 40 °C. van der Waals interactions make major contributions to the adsorption process. Two types of adsorption sites can be identified (Figure 1c), represented by the centers of the density contours. Site I (2 per cage) is located 0.3 nm beneath the center of the six-membered ring. Site II (4 per cage) is also located near the center of the six-ring opening, but with some deviation. The space distribution of these two types of adsorption sites (altogether 6 per cage) results in a tetragonal bipyramid with a nearest neighbor distance of about 0.6 nm.

In light of the above experimental and theoretical results, we used ZIF-8 nanoparticles as fillers, and silicone rubber (polymethylphenylsiloxane, PMPS) as a polymer matrix, to fabricate organophilic pervaporation membranes on the inside surface of alumina capillary substrates by the solution-blending dip-coating method. Figure 2a shows the cross-sectional SEM images of the as-synthesized ZIF-8-PMPS membrane (weight ratio, $W_{ZIF\text{-}8}/W_{PMPS} = 0.10{:}1$). The top-layer thickness is about 2.5 μm, which offers the possibility of achieving a very high permeance (flux normalized by the fugacity driving difference force). The ZIF-8 nanoparticles were embedded in the PMPS phase homogeneously, with no interfacial voids. As shown in the cross-sectional EDXS mapping (Figure 2b), there is a sharp transition between the ZIF-8 nanoparticles (Zn signal) and the substrate (Al signal). The intrusion of PMPS (Si signal) into the substrate pores can be observed, which is advantageous in terms of increasing the stability of the membrane. Both the diffraction peaks related to ZIF-8 and the broad diffuse peaks from the PMPS phase can be observed in the XRD pattern of the ZIF-8-PMPS membrane (Figure 2c).

The as-synthesized ZIF-8-PMPS capillary membrane was sealed in a home-made module and tested for pervaporation recovery of isobutanol from aqueous 1.0–3.0 wt% solutions at 80 °C (see Figure S6 in the Supporting Information). The separation factor of isobutanol over H_2O, calculated as the permeate-to-retentate composition ratio of isobutanol divided by the same ratio for H_2O, ranges from 34.9 to 40.1. Thus, if the feed side of the membrane is exposed to a 1.0 wt% solution of isobutanol from a typical fermentation, the permeate will be around 30 wt% isobutanol. The energy required for pervaporation per unit of isobutanol is only half that of distillation (see Figure S7 and the detailed calculation in the Supporting Information), which indicates that replacing the energy-intensive distillation with the ZIF-8-PMPS membrane pervaporation process would be very profitable. The isobutanol permeance of the ZIF-8-PMPS membrane is 6000–7000 GPU ($1\ \text{GPU} = 1 \times 10^{-6}\ \text{cm}^3\ (\text{STP})\,\text{cm}^{-2}\,\text{s}^{-1}\,\text{cmHg}^{-1}$),

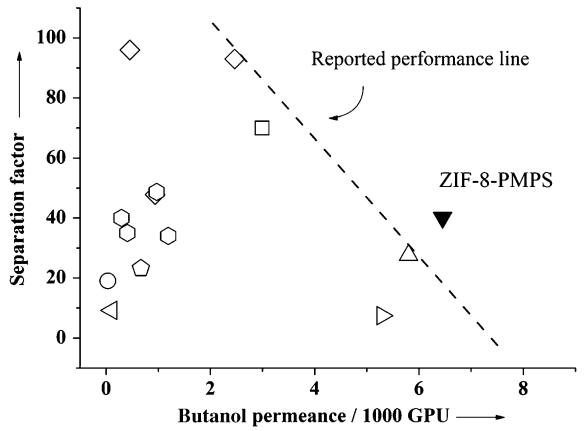

Figure 3. Butanol/H_2O separation factor versus butanol permeance for organophilic pervaporation (OPV) membranes. The dashed line represents the best performance of the state-of-the-art OPV membranes abstracted from Table S1 (1 GPU = 1×10^{-6} cm^3 (STP) cm^{-2} s^{-1} cmHg^{-1}).

which is much higher than the values of reported membranes (Figure 3, see also Table S1 in the Supporting Information). The very high permeance translates into a low membrane area for the recovery of isobutanol per unit weight, thus corresponding to lower capital investment and a smaller footprint, which is a prerequisite for constructing a membrane bioreactor. The separation factor and the high permeance of the ZIF-8-PMPS membrane clearly transcends the upper limit of state-of-the-art OPV membranes (Figure 3), and reaches the economically attractive region.

Both the membrane separation factor and the isobutanol permeability (the product of permeance and membrane thickness) increase simultaneously as the ZIF-8 loading in the composite membrane increases (see Figure S8 in the Supporting Information). This phenomenon corresponds to the desired result that the ZIF-8 nanoparticles can create preferential pathways for isobutanol molecules by virtue of their ultrahigh adsorption selectivity. The separation factor, which decreases at high ZIF-8 loading ($W_{ZIF\text{-}8}/W_{PMPS}$ = 0.20:1), is an exception, which could be attributed to poor filler dispersion (see Figure S9 in the Supporting Information).

ZIF-7 (Zn(benzimidazolate)$_2$, see Figure S10 in the Supporting Information) has the same sodalite-like topology and superhydrophobicity as ZIF-8, but the isotherms of ZIF-7 nanoparticles show insignificant adsorption of isobutanol (see Figure S11 in the Supporting Information). This can be attributed to adsorption on the external surface. No gate-opening effect was observed within the pressure range used in the present study, possibly because of the narrower aperture size of ZIF-7 (0.30 nm)[5] and its much more rigid framework.[21] For comparison, a ZIF-7-PMPS membrane was prepared by the same procedure. The as-synthesized membrane showed a lower separation factor and a lower isobutanol permeance compared with the ZIF-8-PMPS membrane (see Table S1 in the Supporting Information). This finding also demonstrates that the hydrophobic channels of these ZIF-8 nanoparticles made a significant contribution to the selective permeation of isobutanol molecules.

Besides isobutanol, the ZIF-8-PMPS membrane exhibited higher selectivity and productivity for recovering other bio-alcohols from water compared with the pure PMPS membrane (Figure 4). The pervaporation performance increases

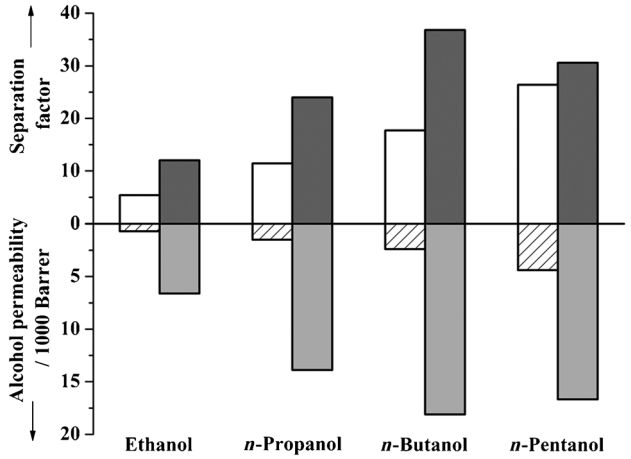

Figure 4. Separation factor and alcohol permeability of PMPS (open and line filled columns) and ZIF-8-PMPS (gray and light gray columns) membranes for aqueous solutions of C_2–C_5 alcohols (1.0 wt% alcohols, 80 °C). 1 Barrer = 1×10^{-10} cm^3 (STP) cm cm^{-2} s^{-1} cmHg^{-1}.

with the carbon number of the alcohols because of the increased adsorption selectivity and capacity. The decrease in separation factor and permeability for *n*-pentanol is characteristic of the interplay of adsorption and diffusion effects. In addition, despite the larger aperture size of silicalite-1 zeolite compared with ZIF-8 (0.55 nm versus 0.34 nm), silicalite-1 membrane shows a monotonic decrease in the alcohol permeability and a noticeable cut-off between C_3 and C_4 alcohols (see Figure S12 in the Supporting Information) as a consequence of its very rigid framework compared to the relatively flexible framework of ZIF-8. The present study shows that the dynamic structural behavior of ZIF materials makes them superior to traditional zeolites in terms of pervaporation, especially for bulky molecules.

In conclusion, as a consequence of the flexible pore apertures and the superhydrophobic pore surface, ZIF-8 nanoparticles exhibit exceptional adsorption selectivity and capacity toward isobutanol molecules, and show a reversible gate-opening effect upon variation of the isobutanol pressure or temperature. As demonstrated by CB-GCMC simulations, each sodalite cage of ZIF-8 can accommodate six isobutanol molecules at 3.5 kPa. These experimental and theoretical observations encouraged us to incorporate ZIF-8 nanoparticles in silicone rubber (PMPS) membranes to fabricate organophilic pervaporation (OPV) membranes. The ZIF-8-PMPS membrane shows a very promising performance for recovering bio-alcohols from dilute aqueous solution, and offers significant potential for the construction of a membrane reactor for in situ product recovery (ISPR) applications. Both the membrane selectivity and permeability can be improved by increasing the ZIF-8 loading in the composite membrane. It is, therefore, expected that polycrystalline ZIF-

8 membranes will show much better performance. As demonstrated in the present study, and considering the very versatile architectures and customizable chemical functionalities of MOF materials, as well as the recent advances in controllable synthesis of MOF membranes, it is believed that the unique properties of MOF materials will offer a new perspective on pervaporation membranes.

Experimental Section

Alumina capillary tubes (3.7 mm OD, 2.4 mm ID, 6.0 cm length, Hyflux Ltd.) were used as supports. The pore size of the inner surface was 40 nm. The as-synthesized ZIF-8 nanoparticles were re-dispersed in isooctane (Kermel, AR) using a probe-type sonicator (AiDaPu) with the horn immersed in the sample for 10 min in an ice bath. This solution (4.5 wt%) was then allowed to warm to room temperature. The catalyst (dibutyltin dilaurate, Shanghai Resin Factory Co., Ltd.), curing agent (Tetraethyl orthosilicate, Kermel, AR), isooctane, PMPS (Shanghai Resin Factory Co., Ltd.), and the above ZIF-8 isooctane solution were added successively to a glass bottle to give the weight composition: catalyst/TEOS/PMPS/ZIF-8/isooctane = 1:10:100:10:333. This mixture was sonicated for 5 min in an ice bath using a probe-type sonicator. The resulting homogeneous mixture was then kept at room temperature for 10 min. The capillary tube was then dip coated into this mixture for 10 s and withdrawn at a speed of 1 mm s^{-1} using an automatic dip coator (WPTL0.01). The membrane was cured at 25 °C for 24 h, 100 °C for 12 h, and then kept at 100 °C for another 12 h under vacuum. By trial and error, several key steps to achieve a homogeneous dispersion were identified: a) freshly synthesized ZIF-8 nanoparticles should be used; b) before mixing with PMPS, the gel-like nanoparticles should be predispersed in isooctane; c) a probe-type sonicator should be adopted instead of an ultrasonic bath.

More experimental and characterization details (e.g. adsorption measurements and simulations, SEM, EDXS, XRD, and pervaporation measurements) are described in the Supporting Information.

Received: June 24, 2011
Published online: September 5, 2011

Keywords: bio-alcohols · membranes · organic–inorganic hybrid composites · pervaporation

[1] a) O. M. Yaghi, M. O'Keeffe, N. W. Ockwig, H. K. Chae, M. Eddaoudi, J. Kim, *Nature* **2003**, *423*, 705; b) S. L. James, *Chem. Soc. Rev.* **2003**, *32*, 276; c) S. Kitagawa, R. Kitaura, S. Noro, *Angew. Chem.* **2004**, *116*, 2388; *Angew. Chem. Int. Ed.* **2004**, *43*, 2334; d) G. Feréy, *Chem. Soc. Rev.* **2008**, *37*, 191.

[2] a) J. R. Li, R. J. Kuppler, H. C. Zhou, *Chem. Soc. Rev.* **2009**, *38*, 1477; b) O. Shekhah, J. Liu, R. A. Fischer, C. Wöll, *Chem. Soc. Rev.* **2011**, *40*, 1081; c) S. T. Meek, J. A. Greathouse, M. D. Allendorf, *Adv. Mater.* **2011**, *23*, 249.

[3] a) H. Bux, F. Liang, Y. Li, J. Crabillon, M. Wiebcke, J. Caro, *J. Am. Chem. Soc.* **2009**, *131*, 16000; b) H. Bux, C. Chmelik, J. M. van Baten, R. Krishna, J. Caro, *Adv. Mater.* **2010**, *22*, 4741; c) Y. S. Li, F. Y. Liang, H. Bux. A. Feldhoff, W. S. Yang, J. Caro, *Angew. Chem.* **2010**, *122*, 558; *Angew. Chem. Int. Ed.* **2010**, *49*, 548; d) Y. S. Li, H. Bux, A. Feldhoff, G. L. Li, W. S. Yang, J. Caro, *Adv. Mater.* **2010**, *22*, 3322; e) H. Guo, G. Zhu, I. J. Hewitt, S. Qiu, *J. Am. Chem. Soc.* **2009**, *131*, 1646; f) R. Ranjan, M. Tsapatsis, *Chem. Mater.* **2009**, *21*, 4920; g) M. C. McCarthy, V. Varela-Guerrero, G. V. Barnett, H. K. Jeong, *Langmuir* **2010**, *26*, 14636; h) Y. Hu, X. Dong, J. Nan, W. Jin, X. Ren, N. Xu, Y. M. Lee, *Chem. Commun.* **2011**, *47*, 737; i) S. R. Venna, M. A. Carreon, *J. Am. Chem. Soc.* **2010**, *132*, 76; j) J. Gascon, S. Aguado, F. Kapteijn, *Microporous Mesoporous Mater.* **2008**, *113*, 132; k) J. Gascon, F. Kapteijn, *Angew. Chem.* **2010**, *122*, 1572; *Angew. Chem. Int. Ed.* **2010**, *49*, 1530.

[4] a) M. J. C. Ordoñez, K. J. Balkus Jr., J. P. Ferraris, I. H. Musselman, *J. Membr. Sci.* **2010**, *361*, 28; b) S. Basu, M. Maes, A. Cano-Odena, L. Alaerts, D. E. D. Vos, I. F. J. Vankelecom, *J. Membr. Sci.* **2009**, *344*, 190; c) K. Díaz, L. Garrido, M. López-González, L. F. del Castillo, E. Riande, *Macromolecules* **2010**, *43*, 316; d) R. Adams, C. Carson, J. Ward, R. Tannenbaum, W. Koros, *Microporous Mesoporous Mater.* **2010**, *131*, 13; e) S. Takamizawa, C. Kachi-Terajima, M. Kohbara, T. Akatsuka, T. Jin, *Chem. Asian J.* **2007**, *2*, 837; f) T. H. Bae, J. S. Lee, W. Qiu, W. J. Koros, C. W. Jones, S. Nair, *Angew. Chem.* **2010**, *122*, 10059; *Angew. Chem. Int. Ed.* **2010**, *49*, 9863; g) B. Zornoza, A. Martinez-Joaristi, P. Serra-Crespo, C. Tellez, J. Coronas, J. Gascon, F. Kapteijn, *Chem. Commun.* **2011**, *47*, 9522.

[5] K. S. Park, Z. Ni, A. P. Côté, J. Y. Choi, R. Huang, F. J. Uribe-Romo, H. K. Chae, M. O'Keeffe, O. M. Yaghi, *Proc. Natl. Acad. Sci. USA* **2006**, *103*, 10186.

[6] X. C. Huang, Y. Y. Lin, J. P. Zhang, X. M. Chen, *Angew. Chem.* **2006**, *118*, 1587; *Angew. Chem. Int. Ed.* **2006**, *45*, 1557.

[7] a) A. Demessence, G. Boissière, D. Grosso, P. Horcajada, C. Serre, G. Feréy, G. J. A. A. Soler-Illia, C. Sanchez, *J. Mater. Chem.* **2010**, *20*, 7676; b) K. Li, D. H. Olson, J. Seidel, T. J. Emge, H. Gong, H. Zeng, J. Li, *J. Am. Chem. Soc.* **2009**, *131*, 10368; c) M. T. Luebbers, T. Wu, L. Shen, R. I. Masel, *Langmuir* **2010**, *26*, 15625.

[8] N. Chang, Z. Y. Gu, X. P. Yan, *J. Am. Chem. Soc.* **2010**, *132*, 13645.

[9] C. Chizallet, S. Lazare, D. Bazer-Bachi, F. Bonnier, V. Lecocq, E. Soyer, A. A. Quoineaud, N. Bats, *J. Am. Chem. Soc.* **2010**, *132*, 12365.

[10] G. Lu, J. T. Hupp, *J. Am. Chem. Soc.* **2010**, *132*, 7832.

[11] a) J. Cravillon, S. Münzer, S. J. Lohmeier, A. Feldhoff, K. Huber, M. Wiebcke, *Chem. Mater.* **2009**, *21*, 1410; b) Y. Pan, Y. Liu, G. Zeng, L. Zhao, Z. Lai, *Chem. Commun.* **2011**, *47*, 2071.

[12] P. Küsgens, M. Rose, I. Senkovska, H. Fröde, A. Henschel, S. Siegle, S. Kaskel, *Microporous Mesoporous Mater.* **2009**, *120*, 325.

[13] a) L. M. Vane, *J. Chem. Technol. Biotechnol.* **2005**, *80*, 603; b) X. Liu, Y. Li, Y. Liu, G. Zhu, J. Liu, W. Yang, *J. Membr. Sci.* **2011**, *369*, 228.

[14] M. E. van Leeuwen, *Fluid Phase Equilib.* **1994**, *99*, 1.

[15] N. Qureshi, M. M. Meagher, R. W. Hutkins, *J. Membr. Sci.* **1999**, *158*, 115.

[16] a) D. Fairen-Jimenez, S. A. Moggach, M. T. Wharmby, P. A. Wright, S. Parsons, T. Düren, *J. Am. Chem. Soc.* **2011**, *133*, 8900; b) C. Gücüyener, J. van den Bergh, J. Gascon, F. Kapteijn, *J. Am. Chem. Soc.* **2010**, *132*, 17704; c) J. Seo, R. Matsuda, H. Sakamoto, C. Bonneau, S. Kitagawa, *J. Am. Chem. Soc.* **2009**, *131*, 12792.

[17] a) D. Frenkel, B. Smit, *Understanding Molecular Simulation: From Algorithms to Applications*, Academic Press, San Diego, **2002**; b) J. I. Siepmann, D. Frenkel, *Mol. Phys.* **1992**, *75*, 59.

[18] A. K. Rappé, C. J. Casewit, K. S. Colwell, W. A. Goddard III, W. M. Skiff, *J. Am. Chem. Soc.* **1992**, *114*, 10024.

[19] A. K. Rappé, W. A. Goddard III, *J. Phys. Chem.* **1991**, *95*, 3358.

[20] W. J. Koros, Y. H. Ma, T. Shimidzu, *Pure Appl. Chem.* **1996**, *68*, 1479.

[21] J. C. Tan, T. D. Bennett, A. K. Cheetham, *Proc. Natl. Acad. Sci. USA* **2010**, *107*, 9938.

